

Paramagnetic Relaxation in Dilute Potassium Ferricyanide*†

ANDREAS RANNESTAD‡ AND PETER E. WAGNER

Department of Electrical Engineering and Carlyle Barton Laboratory, The Johns Hopkins University, Baltimore, Maryland

(Received 4 March 1963)

Paramagnetic relaxation times have been measured for the ground-state doublet of iron present as a dilute substitutional impurity in potassium cobalt cyanide. Measurements were carried out over the temperature range 1.25 to 4.5°K and over a range of Fe/Co concentrations 0.24 to 3.5 at.%. Two frequencies were used, 1.8 and 8.5 Gc/sec, to provide a direct test of the frequency variation of the relaxation time. The "fast-passage-recovery" technique was employed, and a description of the apparatus is included. At 0.24% the 1.8-Gc/sec times are found to be well fitted by a Raman rate $1/T_1 = 4.3 \times 10^{-3} T^9 \text{ sec}^{-1}$ over the entire temperature range and over five decades of time. At 8.5 Gc/sec this rate is augmented by a direct rate $1/T_1 = 3.1 T$. At 0.5% the X-band direct rate is the same, but the Raman rate appears slightly higher; and the L-band rates are substantially faster. All relaxation rates increase with further increases in concentration, but the effect is stronger at 1.8 Gc/sec, so that the rates at both frequencies become equal at 1.7%. Still higher concentrations give rise to behavior not describable by a simple relaxation rate.

For low concentration, the theoretical fourth-power frequency dependence of the direct relaxation process is not verified directly because the low frequency rates are always dominated by the Raman process; however, the frequency dependence must be as at least the third power to be consistent with the data. Some attempts are made to interpret the concentration dependence in terms of cross relaxation between single ions and coupled pairs.

INTRODUCTION

THE subject of electron-spin lattice relaxation in dilute paramagnetic iron-group and rare-earth salts has lately received a great deal of experimental¹⁻⁸ and theoretical⁹⁻¹¹ attention, prompted largely by the comparatively recent appearance of solid-state masers. Various dynamic methods for measuring the relaxation times have been employed with considerable success.^{1,7,8,12} All of them involve the initial application of a strong transient perturbation to a resonance line, after which the line is observed as it decays toward its equilibrium intensity. The techniques, which may be termed "pulse saturation," "fast passage," and "spin-echo," are distinguished chiefly by the nature of the microwave excitation.

Despite the quantity and quality of relaxation time measurements, several rather fundamental features of the theory do not appear to have been given a clear experimental test. There is, for example, scant evidence among iron-group salts for the well-known ninth-power

temperature variation predicted for certain cases,^{9,13} although excellent confirmation has been reported for some of the rare earths.³ In addition, the fourth-power frequency dependence calculated by Van Vleck¹³ for the direct relaxation rate in Kramers doublets has evidently not been verified in iron-group or rare-earth salts. Finally, the variation of the relaxation rate with concentration of the paramagnetic species has not been widely studied.

Iron in potassium cobaltcyanide was chosen for the present work because of several attractive features. The resonance spectrum comes from a well-isolated Kramers doublet and is uncomplicated by hyperfine structure¹⁴; hence, a single line is observed¹⁵ and no difficulties arise from a multiplicity of relaxation paths.¹ Enough is known from crystal field theory to allow quantitative estimates of the energies of the excited doublets from measured g values, so that the likelihood of an Orbach process^{9,10} and a frequency-dependent Raman process¹³ can be reckoned. In addition, past work has shown the relaxation time to vary by many orders of magnitude over a convenient temperature range.^{5,6} Finally, crystals having a wide range of iron concentrations can be prepared by straightforward techniques.

On the other hand, there are certain disadvantages with this material. At relatively modest dilutions the spectrum is complicated by the appearance of extra lines that probably result from exchange between iron ions.^{5,16} In addition, the crystal structure of the host

* Supported in part by the United States Air Force.

† Based on the Doctor of Engineering dissertation of A. Rannestad, School of Engineering Science, The Johns Hopkins University, Baltimore, Maryland.

‡ Present address: Forsvarets Forskningsinstitut, Kjeller pr. Lillistrom, Norway.

¹ J. Castle, P. Chester, and P. Wagner, *Phys. Rev.* **119**, 953 (1960).

² C. Finn, R. Orbach, and M. Wolf, *Proc. Phys. Soc. (London)* **77**, 261 (1961).

³ P. Scott and C. Jeffries, *Phys. Rev.* **127**, 32 (1962).

⁴ R. Ruby, H. Benoit, and C. Jeffries, *Phys. Rev.* **127**, 56 (1962).

⁵ T. Bray, G. Brown, and A. Kiel, *Phys. Rev.* **127**, 730 (1962).

⁶ D. Paxman, *Proc. Phys. Soc. (London)* **78**, 180 (1961).

⁷ W. Mims, K. Nassau, and J. McGee, *Phys. Rev.* **123**, 2059 (1961).

⁸ J. Cowen and D. Kaplan, *Phys. Rev.* **124**, 1098 (1961).

⁹ R. Orbach, *Proc. Phys. Soc. (London)* **77**, 821 (1961).

¹⁰ R. Orbach, *Proc. Roy. Soc. (London)* **A264**, 458 (1961).

¹¹ R. Mattuck and M. Strandberg, *Phys. Rev.* **119**, 1204 (1960).

¹² C. Davis, M. Strandberg, and R. Kyhl, *Phys. Rev.* **111**, 1268 (1958).

¹³ J. Van Vleck, *Phys. Rev.* **57**, 426 (1940).

¹⁴ J. Baker, B. Bleaney, and K. Bowers, *Proc. Phys. Soc. (London)* **B69**, 1205 (1956).

¹⁵ There are actually two lines coming from two orientations of the $\text{Fe}(\text{CN})_6$ complex relative to the macroscopic axes. In the present work the Zeeman field was oriented in a direction for which the two sites are magnetically equivalent.

¹⁶ T. Ohtsuka, *J. Phys. Soc. Japan* **15**, 939 (1960).

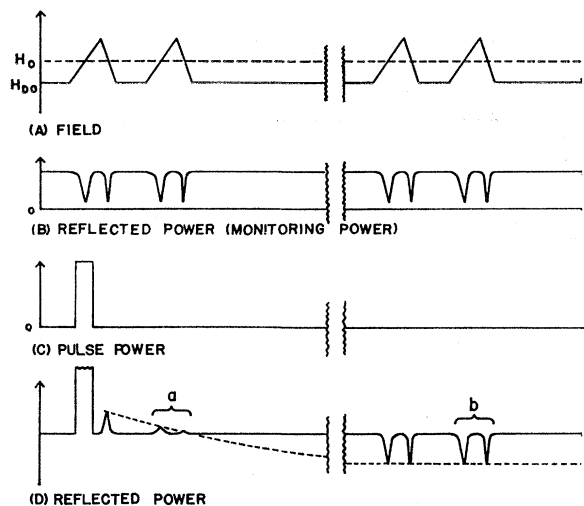


FIG. 1. Time sequence used for fast-passage recovery method of measuring relaxation time. In practice, signals *a* and *b* are superposed on the oscilloscope.

is not simple, rendering almost unattainable a quantitative understanding of the phonon spectrum.

The object of the work reported herein was to measure the spin-lattice time as a function of temperature at two widely different Zeeman frequencies. In accord with the Van Vleck theory,¹³ we anticipated a strong frequency shift for the direct rate and essentially none for the Raman rate, at least at low iron concentration. Such behavior was, in fact, observed. An unexpectedly large concentration dependence was also found and some attempts were made to construct a model for it.

THEORETICAL BACKGROUND

A. Crystal Field Energies

As is well known, Fe^{3+} in the cyanide complex has low spin, that is, the crystal field overrides the Russell-Saunders coupling of the free ion and, in the cubic approximation, leaves a single unoccupied t_2 orbital¹⁷ and a net spin of $\frac{1}{2}$. The ground state is $t_2^5 2T_2$ and is complementary to the $t_2^1 2T_2$ state of Ti^{3+} with respect to the filled t_2 shell. There is a distortion from cubic symmetry which can be treated formally as rhombic and which, together with spin-orbit coupling, splits the sixfold degenerate cubic state into three Kramers doublets. Using the procedure outlined by Griffith¹⁷ and the g values measured by Baker *et al.*,¹⁴ Kiel⁵ has computed the energies of the excited doublets. They are found to lie above the ground doublet by 530 and 830 cm^{-1} . The ground state is, therefore, isolated from the others by an energy that is probably well in excess of the Debye value, so that the relaxation process considered by Orbach^{9,10} can safely be disregarded.

B. Paramagnetic Relaxation

The Van Vleck theory of paramagnetic relaxation has recently been re-examined and recast in a form particu-

¹⁷ We follow the notation of J. Griffith, *The Theory of Transition Metal Ions* (Cambridge University Press, New York, 1961).

larly suitable for the present discussion^{9,10}; it, therefore, seems unwarranted to give more than a brief review. The ion-phonon interaction is, of course, taken to occur via thermal modulation of the local crystalline field. The present case is an example of a Kramers salt in which only the lowest doublet is occupied at the temperatures of interest. Here it is important to note that the interaction cannot connect the two states that comprise the transition.

In the "direct" process of relaxation, a resonant phonon is absorbed or emitted by the ion. To obtain a nonvanishing transition probability, one assumes that the Zeeman field mixes states from excited Kramers doublets into the ground state. In the limit $\hbar\omega/kT \ll 1$, which obtains for the present case, the inverse relaxation time is then proportional to the fourth power of Zeeman frequency and the first power of temperature. Two powers of frequency enter from the Zeeman mixing, while two powers of frequency and the temperature dependence arise solely from the properties of the phonons and would be present as well in the case of a non-Kramers transition.

In the "Raman" process the ion undergoes a transition while at the same time an energetic, nonresonant phonon is scattered into another whose frequency is higher or lower by the Zeeman frequency. There are two possibilities. In one, excited Kramers states are mixed into the ground states by the Zeeman field, and the appropriate phonons are created and destroyed by the oscillating crystal field. Since the corresponding operators are present in the same power as the strain, the Hamiltonian for this crystal field must be quadratic in strain in order to act on two phonons. In the other Raman process, the requisite mixing of states is effected by the phonons themselves, and the Zeeman field can be neglected altogether. The dynamic crystal field Hamiltonian need only be linear in strain, but is allowed to act twice by the use of second-order perturbation theory.

For temperatures well below the Debye value, the first Raman process leads to $1/T_1 \propto \omega^2 T^7$, and the second, to $1/T_1 \propto \omega^9 T^9$ where ω is the Zeeman frequency and T

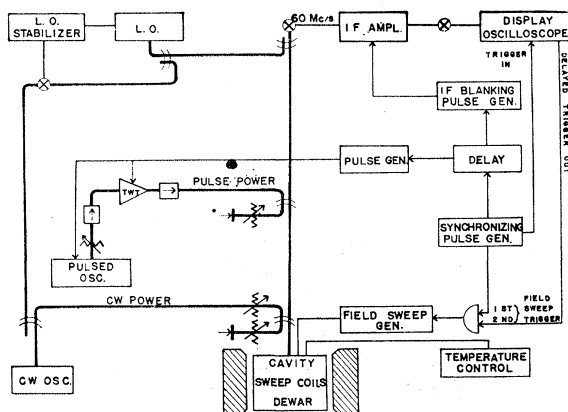


FIG. 2. 1.8 Gc/sec microwave spectrometer.

the temperature. All other things being equal, the second process should dominate the first in the ratio $(kT)^2/(\hbar\omega)^2$, as it is to this order that the squared matrix elements reflect the mixing of states from different Kramers doublets in the two cases.

As pointed out by Orbach, a complication can arise when there are two or more closely spaced excited Kramers doublets. Then the excited states may be mixed among themselves by the Zeeman field, and a field dependence can occur that would otherwise have been absent. The criterion for this *not* to take place is $|H_{\text{Zeeman}}|/(E_3 - E_2) \ll kT/(E_2 - E_1)$, where E_1 , E_2 , and E_3 are, respectively, the energies of the ground and excited doublets, in increasing order. In the present study $|H_{\text{Zeeman}}|/kT \lesssim 0.1$ for our high-frequency results, and $|H_{\text{Zeeman}}|/kT \lesssim 0.04$ for the low-frequency measurements. Taking Kiel's values for the various energy intervals, we find $(E_3 - E_2)/(E_2 - E_1) \approx 0.6$. Hence, our low-frequency data were obtained under conditions well within the above limit, but our high-frequency results were possibly a borderline case.

EXPERIMENTAL APPARATUS AND TECHNIQUES

A. Samples

The $\text{K}_3(\text{Co,Fe})(\text{CN})_6$ crystals were grown from water solution by slow evaporation at a constant temperature. The iron concentrations,¹⁸ in at.%, were: Fe/Co = 0.24, 0.51, 1.0, 1.7, and 3.5%. Two samples were cut from a given crystal, one for measurements at each of the two frequencies employed; the remainder was used for chemical analysis. No particular attention was paid to surface preparation. For all of our measurements the Zeeman field was oriented parallel to the a axis of the crystal¹⁴ and the radio-frequency magnetic field was directed parallel to the b axis.

B. Experimental Method

The microwave resonance method termed "fast-passage recovery" was used throughout. The time sequence was patterned after that of Castle *et al.*¹ and is il-

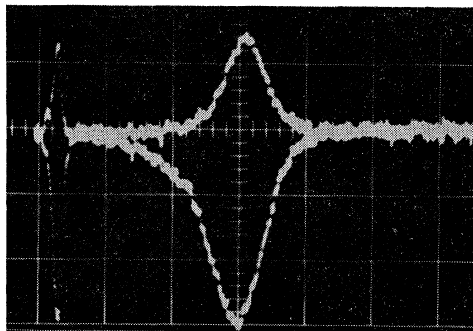


FIG. 3. Inverted line superposed on equilibrium signal. The picture was taken 300 μsec after inversion in 1.0% material, at 1.8 Gc/sec and 1.36°K. The time base is 20 μsec /major division.

¹⁸ Chemical analyses were performed by Spectrochemical Laboratories, Pittsburgh, Pennsylvania.

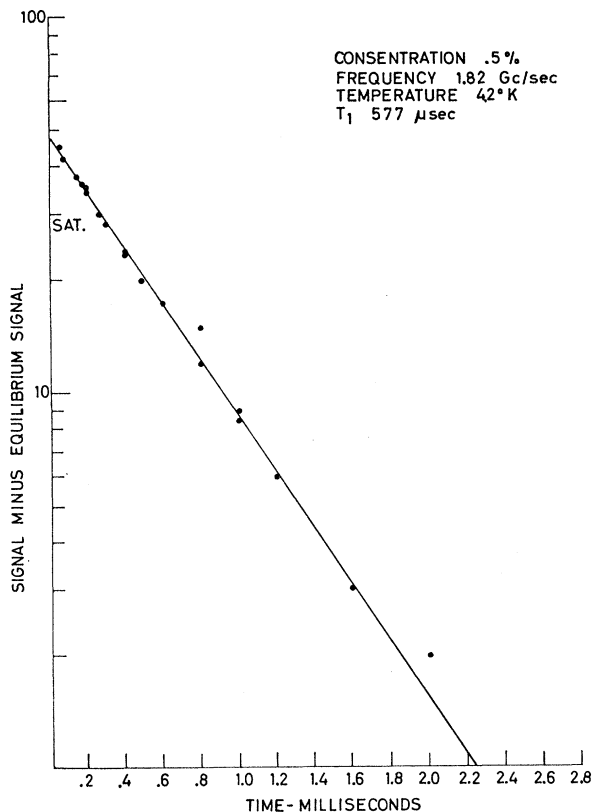


FIG. 4. Semilogarithmic plot of recovery after inversion. Above 30 units (marked "Sat.") the line is inverted.

lustrated in Fig. 1. At a given time the Zeeman field is swept through the resonant value and the line is observed under low monitoring power. If an intense microwave pulse is applied concurrently with the field sweep, the line will be uniformly excited; in fact, under favorable circumstances, viz., a pulse power well in excess of the level required for steady state saturation and a field sweep fast compared to the thermal relaxation time,¹⁹ the line will become emissive. A later application of a second field sweep without the pulse allows observation of the line during the course of its recovery.

The relative advantages of this technique have been discussed elsewhere.¹ The uniform excitation automatically eliminates complications introduced by spin diffusion in inhomogeneously broadened lines. A relatively large monitoring power can be tolerated without itself disturbing the line. Finally, when the line can be inverted a sensitive test for phonon imprisonment is provided.¹

C. Apparatus

Two spectrometers that differed only in nonessential features were built, one for X band and one for L band. The nonmicrowave components were shared. A block diagram applicable to either system is shown in Fig. 2 and is largely self-explanatory. Superheterodyne detec-

¹⁹ A. Redfield, Phys. Rev. 98, 1787 (1955).

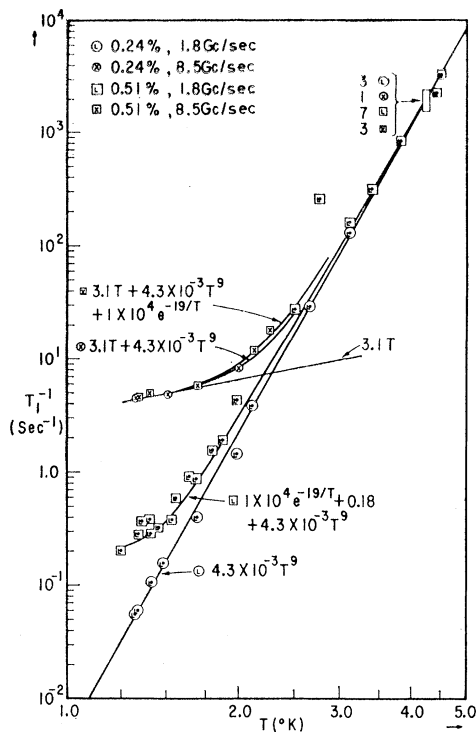


FIG. 5. Log-log plot of relaxation time versus temperature for 0.24 and 0.51% and for both frequencies. Smooth curves have been fitted by the functions indicated.

tion was used, and the local oscillator was frequency locked to the cw oscillator by means of an amplifier-discriminator chain that applied a correction voltage to the reflector of the local oscillator klystron.

Both cw and pulsed microwave power were introduced into the line leading to the cavity via similar microwave bridges that incorporated bidirectional couplers instead of the more conventional magic tee or circulator. Either the in-phase or the quadrature component of microwave susceptibility could be observed by properly balancing the "cw power" bridge, while the "pulse power" bridge could be adjusted independently of the other to null the net power incident on the mixer. Although a 40-dB reduction was thereby attained, the i.f. amplifier was still saturated by the remainder of the pulse, and blanking had to be introduced into the cathodes of four stages of the amplifier in order to speed up its recovery.

Pulsed power was derived from an ITT type F-6868 traveling wave amplifier at *L* band, and from an ITT type F-6996 traveling wave tube at *X* band. In each case the amplifier was gated by the application of a pulse to its current-controlling electrode. Because the *L*-band tube suffered excessive microwave leakage in its "off" condition, a separate pulsed oscillator was used to drive it. At *X* band this problem did not arise, and the traveling wave amplifier was driven by power coupled from the cw "master" oscillator of the spectrometer.

Continuous wave monitoring power at *L* band was

obtained from a General Radio Unit Oscillator, type 1218A, for which frequency stabilization was found to be unnecessary. At *X* band an ITT traveling wave amplifier, type D-2037, was used as an oscillator. External feedback was provided through a high *Q* tunable transmission cavity.²⁰ Although rather touchy to get into operation, the arrangement was found to be extremely stable, presumably because the feedback loop was entirely passive and the only bandwidth limiting element was the reference cavity.

Sample cavities for both frequencies were made out of Hysol 4285 cast epoxy resin and silver plated. At *X* band the dominant rectangular waveguide mode was used. At *L* band, a foreshortened coaxial mode was employed because of size limitations. A length of rectangular line²¹ was chosen to be inductive and was capacitively terminated. To facilitate heat contact, liquid helium was permitted to circulate around the sample inside the cavities; however, inserts made out of foam were placed in the cavities to deflect helium away from regions of strong electric field and, thus, reduce the detuning effect of bubbles.

A Helmholtz pair was attached to each cavity to provide the requisite field sweeps. Two complete field sweeps were used, one for excitation and the other for inspection, as shown in Fig. 1.

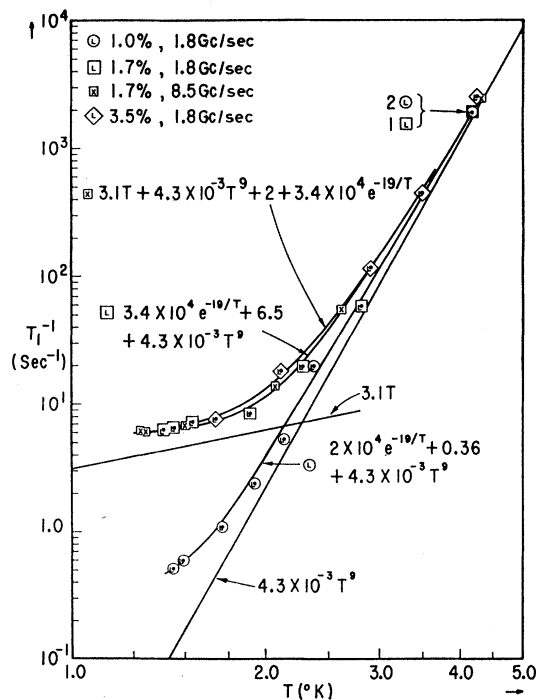


FIG. 6. Log-log plot of relaxation time for concentrations between 1.0 and 3.5%. Smooth curves have been fitted to all except the 3.5% data by the functions indicated.

²⁰ G. Hetland and R. Buss, IRE (Inst. Radio Engrs.), Trans. Electron Devices **1**, 1 (1954).

²¹ Y. Omar and C. Miller, Trans. Am. Inst. Elec. Engrs. **71**, 1 (1952).

TABLE I. Spin-lattice relaxation times.

Concentration (%)	Frequency (Gc/sec)	Temp (°K)	T_1 (msec)	Concentration (%)	Frequency (Gc/sec)	Temp (°K)	T_1 (msec)		
0.24	1.8	4.26	0.655	0.51	1.8	1.34	3.50×10^3		
		4.25	0.460			1.24	4.85×10^3		
		4.25	0.460						
						8.5	4.25	0.425	
						4.25	0.475		
						4.25	0.500		
						2.26	55		
						2.12	83		
						1.70	185		
						1.40	205		
						1.34	221		
						1.04	1.8	~4.18	0.535
						4.18	0.540		
		2.38	50.8						
		2.14	193						
		1.92	428						
		1.71	940						
		1.49	1.7×10^3						
		1.44	1.95×10^3						
0.51	1.8	4.50	0.307	1.7	1.8	4.18	0.540		
		4.40	0.447						
		4.29	0.463						
		4.22	0.530						
		~4.20	0.541						
		~4.20	0.567			2.82	17.6		
		~4.20	0.577			2.28	51		
		~4.20	0.593			1.90	119 ^a		
		4.24	0.530			1.54	140 ^a		
		4.19	0.620			1.40	158 ^a		
		3.82	1.21			1.39	162 ^a		
		3.41	3.23						
		3.11	6.25						
		2.76	3.83						
		2.51	37.4						
		1.98	232						
		1.88	530						
		1.80	650						
						1.69	1.16×10^3		
						1.64	1.10×10^3		
						1.55	1.70×10^3		
						1.53	2.60×10^3		
						1.54	3.00×10^3		
						1.41	3.50×10^3		
		1.40	2.60×10^3						
		1.36	2.70×10^3						
				~3.5	1.8	4.26	0.400		
						3.49	2.3		
						2.90	8.8 ^a		
						2.12	55 ^b		
						1.68	130 ^b		

^a Decay slightly nonexponential.

^b Badly nonexponential decay; asymptotic time constant.

The temperature was varied by pumping on the liquid helium bath and was stabilized by a servo system that added a controlled amount of current to a resistance heater in the bath. A calibrated Allen Bradley resistor was used for temperature measurements.

The following are representative values of the important experimental parameters. Unless otherwise noted, the entries are meant to apply at both frequencies: *L*-band frequency, 1.8 Gc/sec; *X*-band frequency, 8.5 Gc/sec; Monitoring power $\leq 1 \mu\text{W}$; pulsed power $\approx 7 \text{ W}$; temperature range, 1.25 to 4.5°K; maximum field sweep amplitude, 100 G; field sweep rate $\approx 1 \text{ G}/\mu\text{sec}$; field sweep duration $\approx 50 \mu\text{sec}$; minimum measurable time $\approx 50 \mu\text{sec}$.

Figure 3 shows a typical oscilloscope picture of an inverted line superposed on the equilibrium absorption

signal, i.e., a superposition of *a* and *b* of Fig. 1. From traces of this kind taken at various times after excitation, the deviation of the resonance line from its equilibrium height was measured and plotted to give recovery curves like that of Fig. 4. Apart from the exceptions noted below, the decay curves were linear on semilogarithmic plots when the repetition rate was held below one fifth of an inverse time constant and the monitoring power was maintained low enough to avoid obvious saturation of the line during inspection.

RESULTS

A. Relaxation Times

All of the measured relaxation times are listed in Table I and plotted in Figs. 5 and 6. The data are

TABLE II. Paramagnetic resonance spectra of $K_3[Co,Fe](CN)_6$.

Concentration (%) H_0 in G	3.5	0.51 ^a	0.24 ^b	
	Relative intensity ^c			
240	1.0			~20 G wide
280	0.25			
309	0.25			
360	1.0			
390	2.0			
472	1.5			
562		1.10 ⁻⁴		
595	100			Main Line ~15 G wide
621		100		Main Line ~7.5 G wide
625			100	Main Line ~6 G wide
642	1.5			
725		1.10 ⁻⁴		
764	1.0			
828	1.5			

^a At 0.51%, some additional lines having absorption derivatives $<10^{-6}$ that of the main line were seen but their positions were not recorded.

^b At 0.24% lines having absorption derivatives 3×10^{-6} that of the main line would have been observed.

^c Peak-to-peak derivative signal between inflection points, in %.

separated by concentration rather than frequency as an aid in interpretation. The errors in measurement varied considerably; the over-all reliability of the time constants in Table I was about $\pm 10\%$ and was limited chiefly by uncertainty in the logarithmic slopes of the decay curves. Day-to-day reproducibility wherever checked was found to be well within 10%, with one unfortunate exception; data taken two months apart on one of the samples (0.51%, *L* band) differed significantly, as indicated by the scatter evident in Fig. 5 below 1.7°K. A third trial yielded points that extrapolated directly from the first and disagreed with the second trial. At any rate, no points were rejected.

B. Paramagnetic Spectra

The salient features of the spectra of samples representing extremes of concentration are given in Table II. These measurements were taken at 1.8 Gc/sec and 2°K. Up to 0.51%, none of the extraneous lines reported by others^{5,16} was observed at derivative intensities $\geq 10^{-6}$ that of the central line. At 0.24%, rotation of the magnet out of the *a*-axis orientation resulted in two *pairs* of lines rather than just two lines. The splitting of either pair may have been due to polytypism²² but is probably unimportant for the present work.

INTERPRETATION

A. The Low Concentrations

At the lowest concentration and at 1.8 Gc/sec, the data clearly show a Raman decay rate varying as the ninth power of temperature over the entire temperature range and over nearly five decades of time constant. The smooth curve drawn through the experimental points is $1/T_{1L} = 4.3 \times 10^{-3} T^9 \text{ sec}^{-1}$. For 0.24%, the 8.5 Gc/sec rates could be fitted satisfactorily by $1/T_{1X}$

²² J. Artman, J. Murphy, J. Kohn, and W. Townes, Phys. Rev. Letters 4, 607 (1960).

$= 3.1T + 4.3 \times 10^{-3} T^9 \text{ sec}^{-1}$. For 0.51% and 8.5 Gc/sec the low-temperature asymptote also appeared to be $3.1T$, but the relaxation rate appeared to be slightly too high in the transition zone between direct and Raman regions to fit the full 0.24% curve. In this connection it is worth mentioning that only a few points were measured at *X* band in the Raman region; thus, it is possible that the Raman rate could have contained a component other than pure T^9 . More accurate investigation did not seem worthwhile, as at *X* band the Raman rate could predominate at best only over roughly two decades of time. Enough points were measured, however, to establish the absence of a drastic frequency shift at low concentration.

It is interesting to speculate on the weakest frequency dependence of the direct process that could have led to a perceptible deviation from the Raman rate at *L* band, at 0.24% and at the lowest temperatures. By extrapolation from *X* band, a third-power frequency variation would result in an *L*-band direct rate of $\approx 4 \times 10^{-2} \text{ sec}^{-1}$ at 1.3°K. A deviation of this magnitude would be clearly seen in Fig. 5; therefore, while the anticipated fourth-power frequency dependence was not verified, we can at least say that the exponent in question is greater than 3.

B. Concentration Dependence

An unexpectedly strong increase with increasing concentration was found for the relaxation rates at 1.8 Gc/sec and at low temperatures. A more modest shift in the same direction was encountered at *X* band. At a concentration of 1.7%, the relaxation rate had the same values at both frequencies; and at still higher concentration the decay curves ceased to be simple exponentials (at low temperatures), although the asymptotic time constants did not increase greatly over their 1.7% values. The data of Paxman⁶ and of Bray *et al.*⁵ seem to show that there is no profound change with concentration up to 6%, although in both reports there is room in the scatter for some concentration dependence, and Paxman, in fact, takes note of a concentration shift.

A number of mechanisms can give rise to a concentration shift, however, no one of the models we have considered seems wholly convincing. In the first place it is possible that the strain introduced by substituting iron for cobalt is sufficient to alter the local crystalline field. Baker *et al.*¹⁴ and Bleaney and O'Brien²³ have reported a difference in the direction of maximum *g* for dilute and for concentrated ferricyanide, which they interpret as being due to a shift in crystal-field parameters. Strain could alter the coefficients of the direct and Raman rates and could even introduce a field dependent Raman rate with a temperature variation lower than T^9 . All of our data can, in fact, be fitted well with general power series of the form $AT + BT^7 + CT^9$ with constants *A* and *B* adjustable for each concentration and fre-

²³ B. Bleaney and M. O'Brien, Proc. Phys. Soc. (London) B69, 1216 (1956).

quency; however, the A do not vary as the fourth power of frequency (A is obviously independent of frequency at 1.7%) as should be required by the persistence of Kramers degeneracy even in the presence of strain.

Another possibility involves cross relaxation between isolated iron ions and a second species having a different relaxation time. Since paramagnetic impurities do not appear to be present in sufficient number, the alien species must come from the iron itself, probably in the form of exchange-coupled pairs.

The rate equations for cross relaxation between two species may be written

$$\begin{aligned} d\delta/dt &= -a(\delta - \delta_e) - w(N\delta - n\Delta), \\ d\Delta/dt &= -a(\Delta - \Delta_e) - w(n\Delta - N\delta), \end{aligned}$$

where small letters denote one species, taken to be the single ions, and capital letters signify the second species. Δ , δ are the population differences, A , a are the spin lattice rates, and N , n the number of each species. The cross relaxation rate is w , and the subscript labels thermal equilibrium values. The general solution to the decay of Δ , δ after application of a perturbation contains two time constants,

$$2\lambda^\pm = A + a + w(n + N) \pm \{ (A - a)^2 + w^2(n + N)^2 + 2w(n - N)(A - a) \}^{1/2}.$$

If the transitions of the two species are roughly coincident in frequency and if the single ions are initially excited while the other species is not, the single-ion line decays according to

$$\frac{d(t)}{d(0)} = \frac{[A - a + w(n - N) + \{ \}^{1/2}] \exp(-\lambda^- t) - [A - a + w(n - N) - \{ \}^{1/2}] \exp(-\lambda^+ t)}{2\{ \}^{1/2}},$$

where $d = \delta - \delta_e$ is the observed signal. With this model the values plotted in Figs. 5 and 6 are, of course, the long decay constants λ^- .

In trying to apply this model we immediately encounter difficulties with the concentration dependence. We let N be the number of pairs that have a transition nearly coincident in frequency with that of the single ions, and consider first the case of low concentration, where $N/n \ll 1$. In this approximation the slow decay constant is $a + wN(A - a)/(wn + A - a)$ and the excitation of the slow decay mode is $1 - w^2nN/(A - a + wn)^2 \cong 1$, so that the deviation from single exponential behavior is small. This limit depends only on the scarcity of the pair species and is independent of the relative magnitudes of wn and $(A - a)$.

Suppose first that $(A - a)$ is predominant. Then $\lambda^- - a \cong wN$ should vary quadratically with concentration, since N should be proportional to the square of the concentration. It does not appear possible to fit the added decay rate at L band and at 0.5 and 1.0% to a quadratic concentration shift, irrespective of the assumed temperature dependence of wN . On the other hand, suppose that $wn \gg |A - a|$. Then $\lambda^- - a \cong (A - a)N/n$ should show a linear shift with concentration. While consistent with the low-temperature L -band rates at 0.5 and 1.0%, this behavior predicts too fast a rate at low temperatures for 0.24% and far too slow a rate for 1.7%. The picture becomes even worse if one attempts to explain the change between 1.0 and 1.7% by letting N/n become comparable with unity. Then, in the limit $wn \gg |A - a|$, it is easily shown that $\lambda^- - a = (A - a)N/(N + n)$, which should become less concentration-dependent at large N ; the tendency, therefore, is in the wrong direction.

Our results can, however, be explained qualitatively if one invokes more than one species to which cross

relaxation can occur. Suppose, as discussed by Gill and Elliott,²⁴ there is a variety of pairs having a number of different coupling energies. Then one, in general, expects an increase in the relaxation rate with concentration, but quantitative estimates do not appear possible except in limiting cases. We first lift the restriction $N \ll n$, which may no longer obtain above 1%. At high temperatures, where the spin lattice rates dominate, we find $\lambda^- - a = \sum_i w_i N_i$, where i labels a particular kind of pair. In the opposite limit the slow decay constant approaches the weighted average of all participating transitions, viz., $\lambda^- = (na + \sum_i N_i A_i)/(n + \sum_i N_i)$. The fast decay rate is $\lambda^+ = w(n + N) + (nA + Na)/(n + N)$ for a single species; for several species there is no single fast decay mode, but over-all internal equilibrium occurs in times of the order of the $w_i N_i$. After excitation of the single-ion line, a quasisteady state is reached for which the signal is $d(1/\lambda^+ \ll t \ll 1/\lambda^-)/d(0) = n/(n + \sum_i N_i)$, after which a decay to $d = 0$ occurs with characteristic time $1/\lambda^-$.

In our study compound exponentials were just seen at 1.7% and were prominent at 3.5%. Figure 7 is representative of low-temperature decay curves for 3.5%. Here, various parameters were changed to ensure that the effect was not instrumental. Decomposing Fig. 7 yields a fast decay rate $\approx 200 \text{ sec}^{-1}$ compared to the slow rate $\lambda^- \approx 18 \text{ sec}^{-1}$, but the curve contains still faster decay modes at short times and does not break down into only two exponentials. At concentrations of this magnitude it may be artificial to break up the system into pairs, as the number of pairs becomes comparable with the number of ions, and higher order clusters may become important. It is, indeed, possible that the

²⁴ J. Gill and R. Elliott, in *Advances in Quantum Electronics*, edited by J. R. Singer (Columbia University Press, New York, 1961), pp. 399-403.

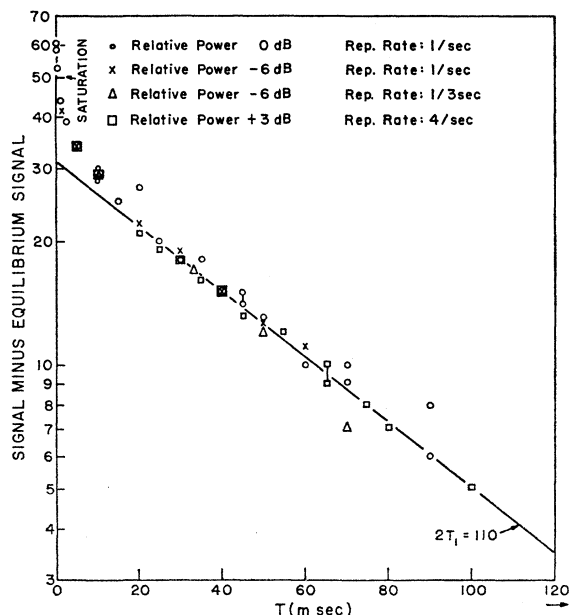


Fig. 7. Semilogarithmic recovery plot for 3.5% material, at 1.8 Gc/sec and 2.12°K. Monitoring power and repetition rate were varied to ensure that the curvature was real; these parameters had been found earlier to introduce spurious curvature under certain conditions.

entire iron sublattice should be treated in a manner that accounts for extensive coupling. In this connection, the "extra" lines that appear in the spectrum at 3.5% are evidently more complicated than might be expected for simple pair spectra.¹⁶

It is probably correct to say that internal equilibrium in the magnetic system occurs in times of the order of a few milliseconds at 3.5%, and the slow rate constant is the weighted average of all the component A_i 's. At higher concentration one should then observe the collective spin lattice relaxation of the entire iron system, and the absence of a strong concentration dependence in the results of Paxman⁶ and Bray *et al.*⁵ is not surprising.

It is interesting to speculate whether there is room in our data for a pair mechanism suggested by Bloembergen and Pershan.²⁵ One assumes fast cross relaxation between ions and the triplet state of pairs that are antiferromagnetically coupled by an exchange energy $J \gg kT$. In this case, for $N \ll n$, the relaxation rate is $\lambda^- = a + (A - a)N/n$ with $N \propto \exp(-J/kT)$ reflecting the thermal occupancy of the triplet state. The spin lattice rate A is essentially independent of T and is assumed much greater than a . We have fitted Figs. 5 and 6 with an added rate that is independent of frequency, proportional to concentration, and exponentially dependent on $1/T$, together with a temperature-independ-

²⁵ N. Bloembergen and P. Pershan, in *Advances in Quantum Electronics*, edited by J. R. Singer (Columbia University Press, New York, 1961), pp. 382-384.

ent rate that is phenomenologically chosen and is supposed to characterize gross cross relaxation apart from the single pair process. (The constant could just as well be proportional to T without degrading the fit.) The exchange energy obtained is $J = 19^\circ\text{K}$; however, the relatively good fits can be taken at best as merely showing consistency with the single pair mechanism, since "gross" cross relaxation could just as easily account for all of the concentration dependence.

SUMMARY AND CONCLUSIONS

At iron concentrations below roughly $\frac{1}{4}\%$, there is little doubt that a pure T^9 Raman rate is predominant at Zeeman frequencies in the L -band region and for temperatures in excess of 1.25°K. There is no significant shift in Raman rate when the frequency is raised by a factor of five, but the direct rate dominates below 2°K at the higher frequency. The direct rate must vary at least as the third power of frequency between 1.8 and 8.5 Gc/sec.

With increasing iron concentration and at low temperatures, the 1.8 Gc/sec relaxation rates increase monotonically up to about 1.7%, while the 8.5 Gc/sec rates increase by a smaller amount. At (and presumably above) this concentration, the rates are the same at both frequencies; and for higher concentration the decays are no longer simple exponentials. The entire concentration dependence is attributed to cross relaxation to coupled pairs or higher order clusters, which themselves relax directly to the lattice in parallel with the relaxation of the single ions.

We feel that further work on concentration-dependent relaxation processes would probably better be carried out on other substances, owing to the rather complicated role played by exchange in our material. At low concentration, however, the substance does show great promise as a near perfect example of a "clean" Kramers system and should for example permit a clear test of the fourth-power frequency dependence expected for the direct process.

ACKNOWLEDGMENTS

The authors are indebted to Dr. J. M. Minkowski for many valuable discussions and in particular for suggesting the material and the design of the L -band cavity. We gratefully acknowledge Dr. A. Kiel's valuable advice. We wish to thank Dr. J. Castle and Dr. D. Feldman of the Westinghouse Research Laboratories for calibrating our temperature sensor, the International Telephone and Telegraph Corporation and in particular A. Hansen for kindly providing the X-band traveling wave amplifier, and J. W. Leight for growing all of our crystals. One of us (A.R.) wishes to acknowledge the generous sponsorship of part of his residence by the Royal Norwegian Air Force.

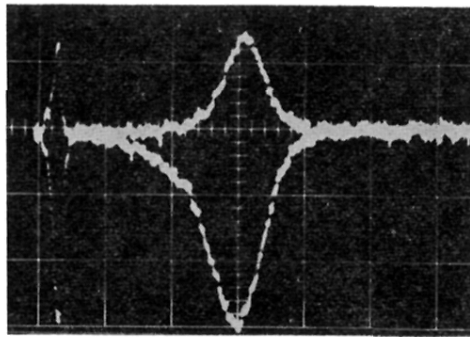


FIG. 3. Inverted line superposed on equilibrium signal. The picture was taken $300\ \mu\text{sec}$ after inversion in 1.0% material, at 1.8 Gc/sec and 1.36°K . The time base is $20\ \mu\text{sec}$ /major division.